AtVPS41-mediated endocytic pathway is essential for pollen tube–stigma interaction in *Arabidopsis*

Lihong Hao[a,1], Jingjing Liu[a,1], Sheng Zhong[a,1], Hongya Gu[a,b], and Li-Jia Qu[a,b,2]

[a]State Key Laboratory for Protein and Plant Gene Research, Peking-Tsinghua Center for Life Sciences, School of Life Sciences, Peking University, Beijing 100871, People's Republic of China; and [b]National Plant Gene Research Center, Beijing 100101, People's Republic of China

Edited by Natasha V. Raikhel, Center for Plant Cell Biology, Riverside, CA, and approved April 26, 2016 (received for review February 24, 2016)

In flowering plants, extensive male–female interactions are required for successful fertilization in which various signaling cascades are involved. Prevacuolar compartments (PVC) and vacuoles are two types of subcellular compartments that terminate signal transduction by sequestrating signaling molecules in yeast and mammalian cells; however, the manner in which they might be involved in male–female interactions in plants is unknown. In this study, we identified *Arabidopsis thaliana* vacuolar protein sorting 41 (AtVPS41), encoded by a single-copy gene with sequence similarity to yeast *Vps41p*, as a new factor controlling pollen tube–stigma interaction. Loss of AtVPS41 function disrupted penetration of pollen tubes into the transmitting tissue and thus led to failed male transmission. In the pollen tubes, AtVPS41 protein is associated with PVCs and the tonoplast. We demonstrate that AtVPS41 is required for the late stage of the endocytic pathway (i.e., endomembrane trafficking from PVCs to vacuoles) because internalization of cell-surface molecules was normal in the *vps41*-deficient pollen tubes, whereas PVC-to-vacuole trafficking was impaired. We further show that the CHCR domain is required for subcellular localization and biological functioning of AtVPS41. These results indicate that the AtVPS41-mediated late stage of the endocytic pathway is essential for pollen tube–stigma interaction in *Arabidopsis*.

VPS41 | pollen tube–stigma interaction | PVC-to-vacuole trafficking | endocytic pathway | *Arabidopsis*

In contrast to the fertilization processes of animals, the sperm cells of which are mobile, the fertilization process in angiosperm plants is more complex and requires more organs to facilitate immotile sperm cells. Pollen grains carrying two sperm cells land on a compatible stigma and, after adhesion and hydration, germinate to form pollen tubes. The germinated pollen tubes then invade the stigma and style, subsequently penetrating into the transmitting tract. Guided by female cues in the transmitting tract tissue, pollen tubes penetrate the septum, climb onto the funiculus, and grow toward the micropyle of the ovule. Two sperm cells are released after the pollen tubes grow into the ovule, after which the sperm fertilize the egg cell and central cell (1–3). During this long process, communication between the male and female gametophytes is very important.

Pollen tube–stigma interaction consists of pollen adhesion, hydration, and germination on the stigma, followed by passaging of growing pollen tubes into the transmitting tract of the style (4). Growth of pollen tubes into the stylar-transmitting tract is an important step in ovule targeting by pollen tubes (4). Pollen tube growth on the stigma is a chemotropic process in which various signaling cascades are involved. Some possible female factors mediating pollen tube–stigma interactions have been identified. Chemocyanin, a small protein, may act as a directional signal on the lily stigma to facilitate entrance of the pollen tube into the style (5). The tobacco glycoprotein, TTS, forms a glycosylation gradient in the transmitting tract, attracting pollen tubes and stimulating pollen tube growth in vivo (6, 7). It is believed that some other female players may also exist, and various signaling pathways are involved in the response of pollen tubes to these directional cues.

Attenuation and termination of signaling activity is an important regulatory mechanism for signaling pathways in animal cells (8, 9). Similar to animal cells, compartmentalization and degradation of signaling molecules, usually mediated by the endocytic pathway, are major regulatory mechanisms in plant cells (10–12). Signaling molecules of extracellular and intracellular origin are degraded in the late stage of the endocytic pathway in which both prevacuolar compartments (PVCs) and vacuoles are involved (13). In mammalian cells, disruption of the late stage of the endocytic pathway often leads to pleiotropic conditions such as immune response deficits, albinism, or neurological disorders (14). However, the manner in which the late stage of the endocytic pathway is involved in regulating signaling pathways during male–female interaction in plants remains unknown.

The endocytic pathway involves cell-surface internalization and PVC-mediated trafficking into vacuoles, which depend mainly on vesicle-mediated transportation. In yeast, studies on vacuolar assembly identified a tethering complex, the homotypic fusion and vacuolar protein sorting (HOPS) complex, which consists of four core subunits and two HOPS-specific subunits, Vps41p and Vps39p (15). Vps41p promotes membrane fusion between late endosomes and lysosomes by working as an effector of Ypt7, a GTP-binding protein (16–18). Loss of Vps41p function led to failure of vacuole membrane fusion and production of fragmented vacuoles (19). Mice lacking *vps41* died early in utero because of impaired down-regulation of growth factor signaling (20). In this study, we report the identification of *Arabidopsis thaliana* vacuolar protein sorting 41 (AtVPS41) as a new factor controlling pollen tube–stigma interaction. Loss of *AtVPS41* function resulted in disrupted penetration of pollen tubes into the transmitting tissue, leading to male gametophytic sterility. We demonstrate that the late stage of the endocytic pathway is impaired in *vps41* pollen tubes. Our results suggest that the AtVPS41-mediated late stage of

Significance

Signaling pathways responsive to both external and internal signals are essential for implementation of biological functions in a cell. After perceiving the signal, the signaling needs to be attenuated and terminated, usually mediated by the endocytic trafficking, to ensure a temporal and spatial control of the signaling activities. In mammals, disruption of the vacuolar protein sorting 41 (VPS41)-mediated endocytic pathway was reported to cause pleiotropic diseases such as neurological disorders. However, the role of the endocytic pathway in plant cells is unknown. We report here that a VPS41-mediated late stage of the endocytic pathway is essential for male–female interaction in *Arabidopsis*.

Author contributions: H.G. and L.-J.Q. designed research; L.H., J.L., and S.Z. performed research; L.H., J.L., S.Z., H.G., and L.-J.Q. analyzed data; and L.H., J.L., S.Z., and L.-J.Q. wrote the paper.

The authors declare no conflict of interest.

This article is a PNAS Direct Submission.

Freely available online through the PNAS open access option.

[1]L.H., J.L., and S.Z. contributed equally to this work.

[2]To whom correspondence should be addressed. Email: qulj@pku.edu.cn.

This article contains supporting information online at www.pnas.org/lookup/suppl/doi:10.1073/pnas.1602757113/-/DCSupplemental.

PLANT BIOLOGY

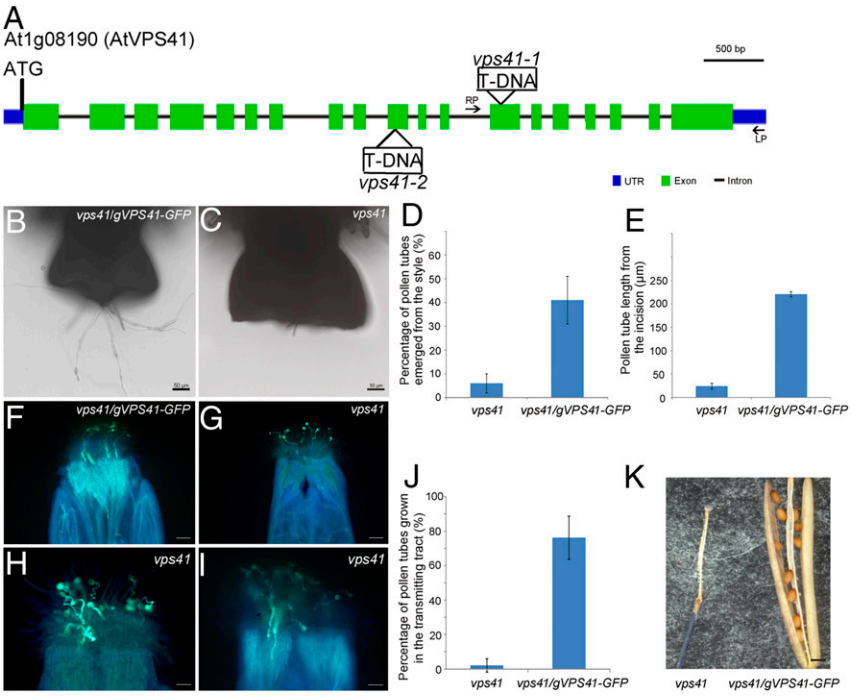

Fig. 1. Phenotype characterization of *vps41* pollen. (*A*) Diagram of T-DNA insertion sites in the two *vps41* alleles. Green box, exons; black line, introns; blue box, untranslated regions. (*B* and *C*) *vps41* pollen and *vps41/gVPS41-GFP* pollen germinated semi-in vivo after hand-limited pollination on the emasculated wild-type stigma. Compared with *vps41/gVPS41-GFP*–complemented pollen tubes, fewer *vps41* pollen tubes penetrated the style. (*D*) Percentage of penetration of *vps41* pollen tubes (n = 70) and *vps41/gVPS41-GFP* pollen tubes (n = 70) into the style 2.5 hag semi-in-vivo. Error bars indicate SD; P value < 0.01. (*E*) Pollen tube length of *vps41* pollen (n = 4) and *vps41/gVPS41-GFP* pollen (n = 29) 2.5 hag semi-in vivo. Error bars indicate SD; P value < 0.01. (*F–I*) Aniline blue staining assay of emasculated wild-type pistils pollinated with *vps41/gVPS41-GFP* pollen (*F*) and *vps41* pollen (*G–I*) 48 h after pollination. (Scale bars: 100 μm in *F* and *G*; 50 μm in *H* and *I*.) (*J*) Bar graph of percentage of pollen tubes growing in the transmitting tract; for *vps41/gVPS41-GFP* pollen, n = 67, and four independent pistils were statistically analyzed; for *vps41* pollen, n = 95; and six independent pistils were statistically analyzed. Error bars indicate SD; P value < 0.01. (*K*) Thirty days after pollination, while there were mature seeds in the siliques pollinated with *vps41/gVPS41-GFP* pollen (*Right*), no seed was seen in the siliques pollinated with *vps41* pollen (*Left*). (Scale bar, 500 μm.)

the endocytic pathway is required for effective pollen tube–stigma interaction in *Arabidopsis*.

Results

Loss of VPS41 Function Results in Failure of Pollen Tube Penetration into the Transmission Tract. To investigate the biological function of VPS41, we obtained two T-DNA alleles of At*VPS41*, *SALK_076372*, and *CS857753*, which were designated *vps41-1* and *vps41-2*, respectively (Fig. 1*A*). We observed a distorted segregation ratio in the progenies of the two mutants, which did not produce homozygotes. Reciprocal cross-analysis revealed that, although the female transmission of the mutant alleles was normal, male transmission was nearly absent (Table 1), suggesting that male function was compromised in *vps41* mutants. We introduced one of the two constructs into *vps41-1* heterozygous mutants, in which the genomic DNA of At*VPS41* was either fused or not fused with *GFP* driven under its native promoter (e.g., Pro_{VPS41}:*VPS41 geDNA* and Pro_{VPS41}:*VPS41 geDNA*-GFP). The male transmission failure phenotype in *vps41-1* was rescued by both constructs (Table 1), demonstrating that the mutation in At*VPS41* (*At1g08190*) was responsible for the phenotype of *vps41* and showing that the VPS41-GFP fusion protein was functional.

We identified complemented plants with a *gVPS41-GFP*$^{+/-}$ *vps41*$^{-/-}$ genotype and collected and separated pollen grains with green fluorescence (complemented) and without green fluorescence (not complemented). Germination of the *vps41-1* mutant pollen grains and *vps41-1* pollen tube growth were similar to the wild type in vitro (Fig. S1). In semi–in vivo germination assays, *vps41-1* mutant pollen grains exhibited normal adhesion and hydration on the stigma (Fig. S2). However, limited pollination assays showed that *vps41-1* mutant pollen tubes barely penetrated into the transmitting tissue of the wild-type stigma, and the number of penetrated *vps41-1* mutant pollen tubes was significantly less than that of penetrated wild-type pollen tubes (Fig. 1 *B–E*). This phenotype was further confirmed by in vivo aniline blue staining assays with the siliques 48 h after pollination (Fig. 1 *F–J*). Hand-pollination of wild-type stigmas with *vps41-1* mutant pollen grains resulted in no seed in the siliques (Fig. 1*K*). These results indicate that, although *vps41-1* pollen tubes are competent to grow in vitro, the mutant pollen tubes cannot penetrate into the transmitting tract of the style.

AtVPS41 Is Localized Mainly in the Late Endosomes/PVCs and Tonoplast in Germinating Pollen Tubes. At*VPS41* was ubiquitously expressed in multiple plant organs and tissues (Fig. S3). To investigate the temporal and spatial expression pattern of At*VPS41* during reproduction, we examined the inflorescences of Pro_{VPS41}:*GUS* and Pro_{VPS1}:*VPS41-GFP* transgenic plants. *VPS41* transcripts were

Table 1. Transmission of the *vps41* alleles through male or female gamete

Parents (♀ × ♂)	Progeny					
	vps41$^{-/-}$	*vps41*$^{+/-}$	*VPS41/VPS41*	Total	TE^F	TE^M
vps41-1$^{+/-}$ selfing	0	209	215	424	NA	NA
vps41-1$^{+/-}$♀ × WT♂		109	111	220	98.20%	NA
WT♀ × *vps41-1*$^{+/-}$♂		4	695	699	NA	0.60%
vps41-2$^{+/-}$ selfing	0	315	334	649	NA	NA
vps41-2$^{+/-}$♀ × WT♂		231	240	471	96.20%	NA
WT♀ × *vps41-2*$^{+/-}$♂		0	405	405	NA	0%
WT♀ × *vps41*$^{+/-}$; Pro_{VPS41}:*VPS41 geDNA*$^{+/+}$♂		275	279	554	NA	98.57%
WT♀ × *vps41*$^{+/-}$; Pro_{VPS41}:*VPS41 geDNA -GFP*$^{+/+}$♂		292	298	590	NA	97.99%

NA, not applicable; TE^F, transmission efficiency of female gametophyte; TE^M, transmission efficiency of male gametophyte.

abundantly detected in mature pollen grains, but not in immature developing pollen (Fig. 2 *A* and *B*). Similarly, the VPS41-GFP signal was observed in mature tricellular pollen, but not in microspores and bicellular pollen. In addition, VPS41-GFP was detected in vegetative cells and sperm cells in pollen tubes (Fig. 2 *C–I*). Interestingly, in sperm cells, the GFP signal formed a ring structure surrounding sperm nuclei (Fig. 2 *D* and *G*).

In the complemented pollen tubes of *gVPS41-GFP*$^{+/-}$ *vps41*$^{-/-}$ plants, the GFP signal was highly dynamic and detected in tubular structures and variably sized endosome-like punctate structures (Movie S1). To determine the subcellular localization of AtVPS41, we crossed *gVPS41-GFP*$^{+/-}$ *vps41*$^{-/-}$ plants with 18 endomembrane marker lines (wave line markers) (21). In the pollen tubes of the F1 progeny plants, the VPS41-GFP signal was colocalized with vacuole marker *Pro*$_{UBQ10}$*:VAMP711-mCherry* (n = 14) and three PVC markers: *Pro*$_{UBQ10}$*:RABG3c-mCherry* (n = 17), *Pro*$_{UBQ10}$*:RABG3f-mCherry* (n = 12), and *Pro*$_{UBQ10}$*:RABF2a-mCherry* (n = 9) (Fig. 2 *J–U*), but not with other markers (Table S1). These results showed that, in germinating pollen tubes, AtVPS41 resided mainly in the late endosomes/PVCs and tonoplast, similar to the localization profile of its homologs in yeast and mammalian cells (22, 23).

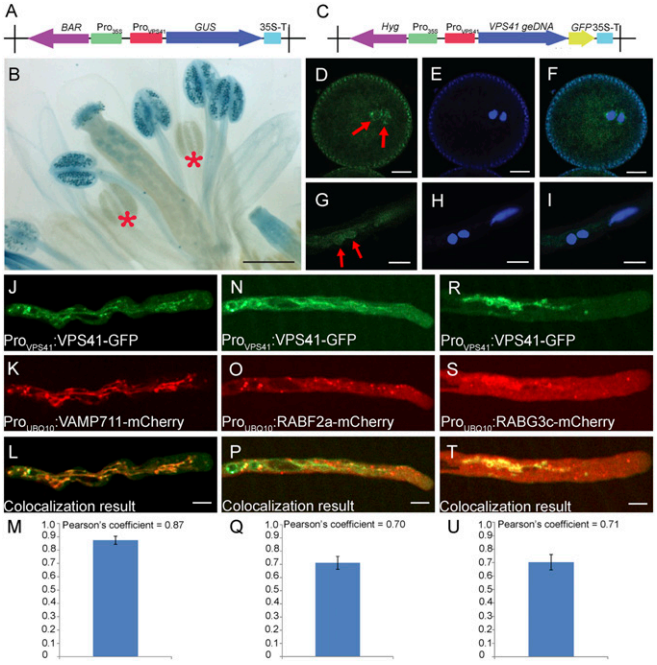

Fig. 2. Expression pattern of VPS41 in floral organs and subcellular localization of VPS41 in pollen tubes. (*A*) Construct diagram of the *Pro*$_{VPS41}$*:GUS* reporter. (*B*) Expression pattern of *VPS41* gene in floral organs revealed by GUS assay. Red stars indicate developing pollen. (Scale bar, 500 μm.) (*C*) Construct diagram of the *Pro*$_{VPS41}$*:VPS41 geDNA-GFP* reporter. (*D–I*) Localization of VPS41 in mature pollen (*D–F*) and germinating pollen tubes (*G–I*) of *Pro*$_{VPS41}$*:VPS41 geDNA-GFP* transgenic plants. (*D* and *G*) GFP signals. (*E* and *H*) DAPI-staining images. (*F* and *I*) Overlay of the GFP and DAPI images. Red arrows indicate sperm cells. (Scale bars, 5 μm.) (*J–M*) Localization of VPS41-GFP fusion protein (*J*) and VAMP711-mCherry fusion protein (*K*) in pollen tubes. (*L*) Colocalization result of VPS41-GFP and VAMP711-mCherry. Pearson's coefficient of the colocalization result in *M*. Fourteen independent pollen tubes were used for statistical analysis. (Scale bar, 10 μm.) (*N–Q*) Localization of VPS41-GFP fusion protein (*N*) and RABF2a-mCherry fusion protein (*O*) in pollen tubes. (*P*) Colocalization result of VPS41-GFP and RABF2a-mCherry. Pearson's coefficient of the colocalization is shown in *Q*. Nine independent pollen tubes were used for statistical analysis. (Scale bar, 10 μm.) (*R–U*) Localization of VPS41-GFP fusion protein (*R*) and RABG3c-mCherry fusion protein (*S*) in pollen tubes. (*T*) Colocalization result of VPS41-GFP and RABG3c-mCherry. Pearson's coefficient of the colocalization is shown in *U*. Seventeen independent pollen tubes were used for statistical analysis. (Scale bar, 10 μm.)

AtVPS41 Is Recruited to PVCs and the Tonoplast by Interacting with RABF2a, RABG3c, and VAMP711. In yeast cells, the HOPS complex is recruited by the active form of RAB GTPase Ypt7/RAB7 to mediate fusion between the prevacuolar compartment membrane and vacuole/lysosome membrane with the assistance of SNARE proteins (16–18). In *Arabidopsis*, RAB7/RABG GTPases and a Rab5 homolog Rha1/RABF2a were also involved in vacuolar trafficking of cargo proteins (24–26). To test whether recruitment of AtVPS41 to PVCs/tonoplast is also mediated by interaction between AtVPS41 and the RAB GTPases and SNARE proteins, we performed split-ubiquitin yeast two-hybrid assays (27, 28) using AtVPS41 as a bait protein and RABF2a, RABG3c, and VAMP711 as prey proteins. As shown in Fig. 3*A*, we found that AtVPS41 interacted with RABF2a, RABG3c, and VAMP711. We further generated constructs of the VPS41-MYC fusion protein and RABF2a-FLAG/RABG3c-FLAG/VAMP711-FLAG and transiently coexpressed them in tobacco (*Nicotiana benthamiana*) leaves by agro-infiltration (29). We found that RABF2a-FLAG, RABG3c-FLAG, and VAMP711-FLAG were coimmunoprecipitated with VPS41 (Fig. 3*B*). Taken together, these results indicate that AtVPS41 is recruited to PVCs by interacting with RAB GTPases RABF2a and RABG3c, whereas AtVPS41 is recruited to the tonoplast through interacting with the SNARE protein VAMP711.

PVC-to-Vacuole Trafficking Is Greatly Impaired in *vps41-1* Pollen Tubes. The dual localization of AtVPS41 in PVCs and vacuoles suggests that AtVPS41 is probably involved in PVC-to-vacuole trafficking in pollen tubes. To verify this hypothesis, we transformed *Pro*$_{LAT52}$*:2S albumin-mRFP*, which encodes a fusion protein to be transported into vacuoles through a PVC-mediated transport pathway in cultured plant cells (30), into *gVPS41-GFP*$^{+/-}$ *vps41*$^{-/-}$ plants. At 1.5 h after germination (hag), the 2S albumin-mRFP signal was found mainly in tonoplast-like tubular membrane structures, as well as in endosome-like punctate structures in complemented pollen tubes (Fig. 4 *A* and *B*), whereas in *vps41-1* mutant pollen tubes the signal was observed mainly in endosome-like punctate structures (Fig. 4 *C* and *D*). At 3.5 hag, the 2S albumin–monomeric red fluorescent protein (mRFP) signal was observed mostly in vacuoles in complemented pollen tubes (Fig. 4 *E* and *F*), whereas in *vps41-1* mutant pollen tubes the mRFP signal was retained mostly in endosome-like structures (Fig. 4 *G* and *H*), suggesting that vacuolar transport of the 2S albumin-mRFP signal was greatly compromised in *vps41-1* mutant pollen tubes.

PVCs and vacuoles are involved in the late stage of the endocytic pathway, which down-regulates signaling activity by sequestrating activated signaling components into degradative organelles (11, 12, 20). To examine endocytic activity in *Arabidopsis* pollen tubes, we treated both the wild-type and *vps41-1* mutant pollen tubes with FM4-64, an endocytic tracer for internalization and endosomal trafficking (31). Uptake and intracellular accumulation of FM4-64 were evident within 10 min in wild-type (n = 50) and *vps41-1* pollen tubes (n = 50) (Fig. 4 *I* and *J*) with clearly labeled endosomes, whereas the endocytosis rates of the groups were statistically indistinguishable (Fig. 4*K*), indicating that the early stage of the endocytic pathway was not affected in *vps41-1* mutant pollen tubes. After 4 h, FM4-64 had accumulated in the tonoplast in most (42/50) of the wild-type pollen tubes, but was still mainly present in punctate endosome-like structures in most (36/50) *vps41-1* mutant pollen tubes (Fig. 4 *L* and *M*). The relative FM4-64 transport to tonoplast was dramatically decreased in *vps41-1* pollen tubes in comparison with the wild-type pollen tubes (Fig. 4*N*). These results demonstrate that loss of AtVPS41 disturbs the late stage of the endocytic pathway in pollen tubes.

The CHCR Domain of AtVPS41 Is Required for Subcellular Localization and Biological Functioning. To determine the importance of each domain of VPS41 for subcellular localization and functioning of the protein, we introduced two truncated forms of AtVPS41, lacking the RING domain or CHCR domain and designated *Pro*$_{VPS41}$*:VPS41 geDNAΔRING*-GFP and *Pro*$_{VPS41}$*:VPS41 geDNAΔCHCR*-GFP, respectively, into *vps41-1*$^{+/-}$ heterozygous mutant plants

PLANT BIOLOGY

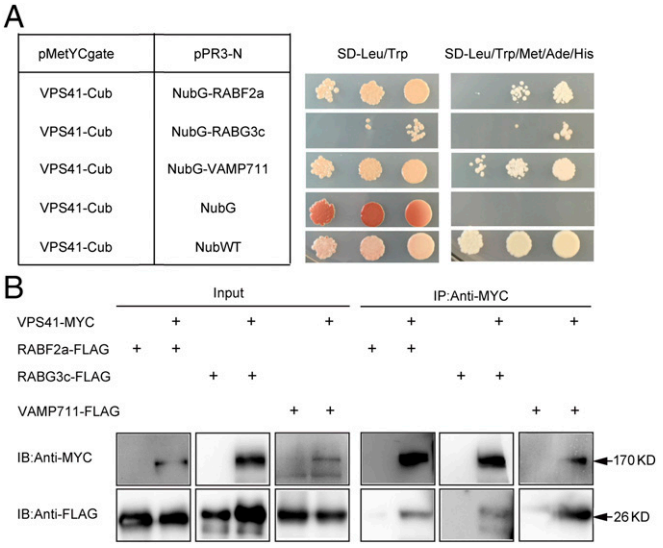

Fig. 3. AtVPS41 interacts with RABG3c, RABF2a, and VAMP711. (*A*) Yeast two-hybrid assays of VPS41 with RABG3c, RABF2a, and VAMP711. NubWT represents the wild-type N-terminal half of ubiquitin. NubG represents the mutated N-terminal half of ubiquitin that was not able to interact with the C-terminal half of ubiquitin. Interactions between two proteins were tested using Met, Ade, and His reporter genes. (*B*) Co-IP assays. VPS41-MYC with RABF2a-FLAG, RABG3c-FLAG, and VAMP711-FLAG were transiently coexpressed in *Nicotiana benthamiana* leaves. Total proteins were subjected to immunoprecipitation with MYC beads followed by immunoblot analysis.

(Fig. 5*A*). Pro_{VPS41}:*VPS41 geDNAΔRING*-GFP$^{+/+}$ *vps41-1*$^{+/-}$ (hereafter, VPS41ΔRING/*vps41-1*$^{+/-}$ complemented plants) and Pro_{VPS41}:*VPS41 geDNAΔCHCR*-GFP$^{+/+}$ *vps41-1*$^{+/-}$ (hereafter, VPS41ΔCHCR/*vps41-1*$^{+/-}$ complemented plants) transgenic T2 plants were crossed with wild-type plants and calculated for the Kan^r/Kan^s ratio in the resulting progeny, which reflected male transmission of the *vps41-1* allele. Whereas pollination with pollen from VPS41ΔRING/*vps41-1*$^{+/-}$–complemented plants produced a Kan^r/Kan^s ratio of almost 1:1 (395:390) in the progeny, pollination with pollen from VPS41ΔCHCR/*vps41-1*$^{+/-}$–complemented plants produced a Kan^r/Kan^s ratio of 0.40:1 (138:347) (Fig. 5*B*). This result indicates that the CHCR domain, but not the RING domain, is required for AtVPS41 to function in male transmission. The VPS41ΔCHCR-GFP signal was partially colocalized with PVC marker RABG3f (21) (n = 3), but not with tonoplast marker VAMP711 (n = 6) (Fig. 5 *C*–*J*). Therefore, the CHCR domain is required for proper localization of AtVPS41 in the tonoplast and for functioning of the protein.

Taken together, our results demonstrate that AtVPS41-mediated PVC-to-vacuole trafficking is an important process in the endocytic pathway in pollen tubes that is essential for pollen tube–stigma interaction in *Arabidopsis* (Fig. 6).

Discussion

Successful fertilization requires extensive pollen–pistil interaction, which occurs immediately after a pollen grain contacts a stigmatic papillae. In this study, we identified AtVPS41 as an essential male factor participating in pollen tube–stigma interaction based on genetic evidence and the results of in vitro and semi-in vivo biological studies. First, *vps41* mutants are male-gametophyte–sterile because of the failure of pollen tubes to penetrate into the transmitting tract of the stigma. Second, VPS41 is dynamically localized in the PVCs and vacuoles in pollen tubes. Third, the late stage of endocytic trafficking is compromised in *vps41* mutant pollen tubes. Fourth, disrupting VPS41 localization in the tonoplast compromised VPS41 function in pollen tubes. Therefore, the AtVPS41-mediated late stage of the endocytic pathway in pollen tubes is essential for pollen tube–stigma interaction in *Arabidopsis*.

Pollen tube growth in pistils is directional and requires extensive cell–cell communication between pollen tubes and pistil tissues, including signal perception at the plasma membrane of pollen tubes, signal transduction into the cytoplasm of pollen tubes, and signaling cue/receptor complex internalization and turnover, in which guidance signal cues from sporophytic and female gametophytic tissues are required and endomembrane trafficking plays an essential role (Fig. 6). Because in mammals loss of *Vps41* resulted in deficient down-regulation of growth factor signaling and thus led to embryonic lethality (20) and because Vps41 is highly conserved among eukaryotes, Vps41 may also be implicated in attenuation of signaling cascades involved in cell–cell communication between pollen tubes and female tissues in *Arabidopsis*. It is very possible that defective

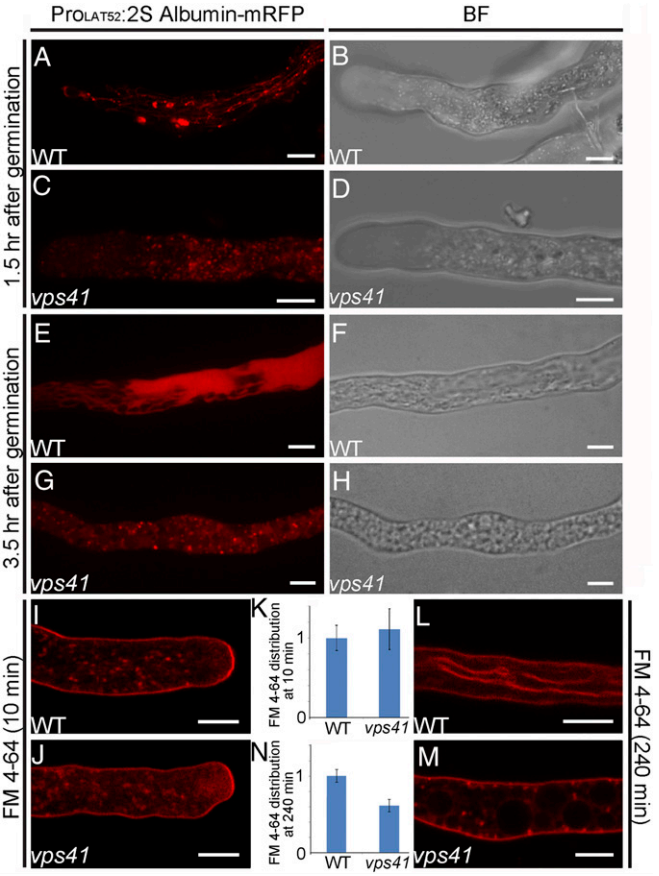

Fig. 4. Endosomal trafficking to vacuoles was greatly compromised in *vps41* pollen tubes. (*A*–*H*) Endosomal trafficking to vacuoles revealed by a 2S albumin–mRFP fusion protein marker. Fluorescent and bright-field images of wild-type and *vps41* pollen tubes are shown. (*A* and *B*) Fluorescent and bright-field images of wild-type pollen tubes at 1.5 hag. (*C* and *D*) Fluorescent and bright-field images of *vps41* pollen tubes at 1.5 hag. (*E* and *F*) Fluorescent and bright-field images of wild-type pollen tubes at 3.5 hag. (*G* and *H*) Fluorescent and bright-field images of *vps41* pollen tubes at 3.5 hag. At least 20 independent pollen tubes were observed for each genotype and each time point. (Scale bar, 5 μm.) (*I*–*M*) FM4-64 uptake assays. Intracellular accumulation of FM4-64 is shown within 10 min after incubation in 5 μM FM4-64 in a wild-type pollen tube (*I*) and *vps41* pollen tube (*J*). (*K*) Statistical quantification of relative FM4-64 uptake within 10 min. At least 50 independent pollen tubes were used for statistical analysis for each genotype. Error bars indicate SD. Distribution of FM4-64 is shown after 240 min of incubation in 5 μM FM4-64 in a wild-type pollen tube (*L*) and a *vps41* pollen tube (*M*). (*N*) Statistical quantification of relative FM4-64 transport to tonoplast at 240 min; 20 independent pollen tubes were used for statistical analysis for *vps41* pollen tubes, and 14 independent pollen tubes were used for statistical analysis for wild-type pollen tubes. (Scale bar, 5 μm.)

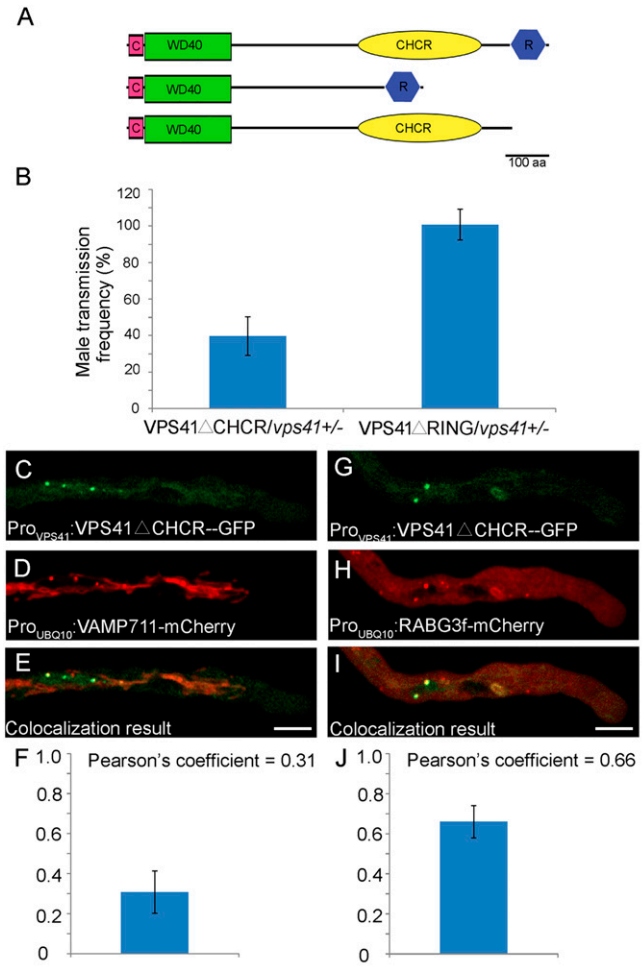

Fig. 5. CHCR domain is essential for subcellular localization and biological function of VPS41. (*A*) Schematic diagram representing full-length and two truncated forms of AtVPS41: VPS41△CHCR and VPS41△RING. (*B*) VPS41△CHCR and VPS41△RING were introduced into *vps41*$^{+/-}$ heterozygous plants. Although the VPS41△RING could fully rescue the male transmission frequency, the VPS41△CHCR could rescue the ratio to only about 40%, indicating that the CHCR domain is essential for the biological function of AtVPS41. Error bars indicate SD. (*C*–*F*) Localization of VPS41△CHCR-GFP fusion protein (*C*) and VAMP△711-mCherry fusion protein (*D*) in pollen tubes. Colocalization result of VPS41△CHCR-GFP and VAMP711-mCherry is shown in *E*. Pearson's coefficient of the colocalization result is shown in *F*. Three independent pollen tubes were statistically analyzed. (Scale bar, 10 μm.) (*G*–*J*) Localization of VPS41CHCR-GFP fusion protein (*G*) and RABG3f-mCherry fusion protein (*H*) in pollen tubes. (*I*) Colocalization result of VPS41△CHCR-GFP and RABG3f-mCherry. Pearson's coefficient of the colocalization result in *J*. Six independent pollen tubes were statistically analyzed. (Scale bar, 10 μm.)

penetration of *vps41* pollen tubes into the stylar-transmitting tract is due to the failure of such pollen tubes to respond to female signal cues that need to be internalized and transported through the AtVPS41-mediated endocytic pathway (Fig. 6). Another possibility, however, also exists: the mutation of *VPS41* might affect the pollen tube growth, the defective phenotype of which is likely masked in vitro by a component of the medium.

Another possible cause is associated with enzymes. After germinating on the stigma, pollen tubes have to penetrate the cuticle covering the stigmatic surface (32–34). Pollen-held enzymes, such as pectin-degrading enzymes and enzymes that modify the cell wall, must be secreted to degrade the stigmatic cuticle and loosen the stigmatic cell wall. For example, serine esterases have been reported to be required for pollen tube penetration into dry *Brassica* stigmas (34). Therefore, it is also possible that AtVPS41 is involved in the regulated release of these enzymes from pollen tubes.

The finding that the CHCR domain of AtVPS41 is needed for proper localization and biological functioning of the protein is consistent with the fact that VPS41 is an essential subunit of the HOPS complex, a tethering complex that mediates heterotypic late endosome vacuole fusion and homotypic vacuolar fusion in yeast and mammalian cells (22). This is also supported by the observation that multiple small vacuoles occurred in the *vps41-1* mutant pollen tubes (Fig. S4), showing that membrane fusion associated with endomembrane trafficking is impaired in such plants. The compromised vacuole biogenesis may affect the buildup of the turgor pressure in *vps41* pollen tubes and consequently affects the pollen tube penetration. In mammalian cells, VPS41 is involved in sorting proteins to the regulated secretory pathway in a process that is also dependent on the CHCR domain, which interacts with adaptor protein 3 (AP-3) (35). This process is highly specific for VPS41 and operates independently of the HOPS complex (35). Therefore, another possibility is that AtVPS41 may also be involved in regulating a secretory pathway independent of the HOPS complex in pollen tubes.

In the present study, we provide evidence demonstrating that AtVPS41-mediated endomembrane trafficking, possibly PVC-to-vacuole trafficking via the endocytic pathway, is essential for pollen tube–stigma interaction in *Arabidopsis*. Future studies should aim to investigate the molecular mechanisms by which AtVPS41 mediates endomembrane trafficking in pollen tubes.

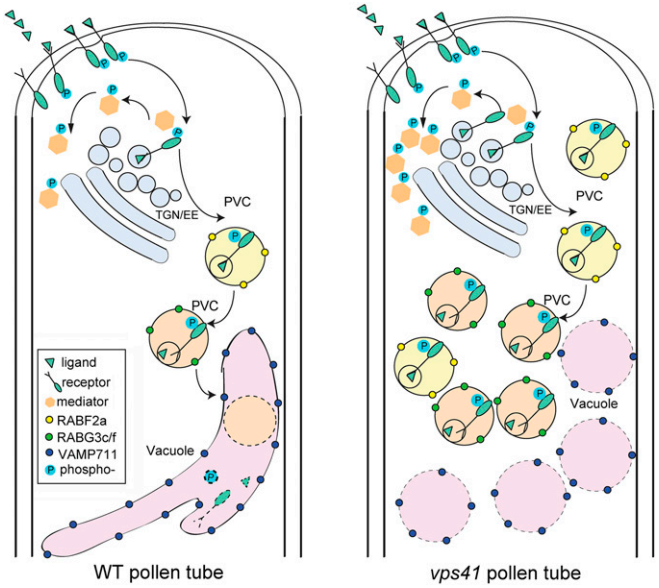

Fig. 6. A proposed model for endocytic endomembrane trafficking of pollen tube plasma membrane-localized receptors and female cues. Upon stimulation with the female cues, the receptors are phosphorylated and then internalized into the trans-Golgi network/early endosome (TGN/EE) where the signals are transmitted to downstream intracellular mediators. The receptors are further delivered to RABF2a-positive PVCs, and through maturation of endosomal organelles, the receptors are transferred into the RABG3c-positive PVCs where the pH is lower and the ligands dissociate with the receptors. Finally, the receptors and ligands are transported into vacuoles for degradation, thus realizing the attenuation of the signaling. In *vps41* pollen tubes, although the internalization of the receptors is normal, the PVC-to-vacuole trafficking of receptors is greatly impaired. Thus, the vacuoles are not assembled normally and the PVC cannot be fused with vacuoles efficiently, which leads to accumulation of PVCs in pollen tubes. Meanwhile, these active receptors may also be accumulated in the TGN/EE, which may cause the excessive signaling in pollen tubes. The deregulated signaling in pollen tubes may eventually result in the failure of pollen tube penetration into the transmitting tract.

Materials and Methods

VPS41 Sequence Analysis. The sequences of VPS41 homologs in various species were obtained from the National Center for Biotechnology Information using BLAST (blast.ncbi.nlm.nih.gov/Blast.cgi). Protein domains were analyzed using the Protein Homology/Analogy Recognition Engine (Phyre) (www.sbg.bio.ic.ac.uk/~phyre/).

Plasmid Construction. To generate the Pro_{VPS41}:*GUS* construct and the Pro_{VPS41}:*VPS41 geDNA* construct for complementation, GATEWAY-compatible destination vector pCB308R or pCB2003 was used, respectively (36). For the Pro_{VPS41}:*VPS41 geDNA*-GFP construct, a reconstructed vector pH7FWG0, which was made from the GATEWAY-compatible destination vector pH7FWG2 (VIB-Ghent University), was used.

Pro_{LAT52}:*γTIP-mCherry* was constructed from the Pro_{35S}:*γTIP-mCherry* construct (The Arabidopsis Information Resource stock no. CD3-975) by replacing the 35S promoter with a LAT52 promoter. For generation of co-immunoprecipitation (Co-IP) constructs, a GATEWAY-compatible pBA-Myc vector was used for Pro_{35S}:*VPS41-6×Myc* construction and a GATEWAY-compatible pB7FLAGWG2 vector was used for Pro_{35S}:*RABF2a/RABG3c/VAMP711-3×FLAG* construction. To generate the Pro_{VPS41}:*VPS41 geDNAΔRING*-GFP construct for complementation assay, the pENTRY-Pro_{VPS41}:*VPS41 geDNAΔRING* and pENTRY-Pro_{VPS41}:*VPS41 geDNAΔCHCR*-GFP plasmids were then cloned into pH7FWG0.

In Vitro Pollen Germination Analysis. In vitro pollen germination assays were conducted according to previously reported protocols (37, 38). The measurement of pollen tube length and pollen tube germination percentages were made with Image J software (rsbweb.nih.gov/ij/).

Semi-in Vivo Pollen Germination Assay, Aniline Blue Staining, and GUS Staining. Semi-in vivo pollen germination assay and aniline blue staining were conducted according to previously reported protocols (39). The histochemical GUS assay was performed according to a reported protocol (40).

FM4-64 Uptake Quantification Assay and Colocalization Analysis. Pollen tubes 2 hag were stained with 5 μM FM4-64 (Molecular Probes) as according to ref. 31. Fluorescence intensities of 50 independent pollen tubes were calculated and standardized for each genotype. Fluorescence images were observed according to a previously reported protocol (41).

Co-IP and Immunoblotting. Co-IP assays were conducted as previously described (42, 43). Immunoblotting was performed as previously described (39) using anti-MYC and anti-FLAG antibody (Santa Cruz).

ACKNOWLEDGMENTS. We thank Dr. Zhenbiao Yang (University of California, Riverside) for suggestions and discussions; Dr. Sheila McCormick (University of California, Berkeley) for the pENTRY-ARA6 and pENTRY-ARA7 plasmids; Dr. Qi Xie (Institute of Genetics and Developmental Biology, China) for the Y2H cDNA library; Dr. Liwen Jiang (Chinese University of Hong Kong) for the plasmid carrying a *2S albumin* gene; Dr. Fred Berger (Temasek Life Sciences, Singapore) for HTR10-mRFP seeds; and Dr. Jerry Kaplan (University of Utah) for the Δ*vps41* yeast strain. This work was supported by the National Basic Research Program of China (Grant 2011CB915402) and the National Natural Science Foundation of China Grant 31370344 (to L.-J.Q.). This work was partially supported by the 111 Project.

1. Lord EM, Russell SD (2002) The mechanisms of pollination and fertilization in plants. *Annu Rev Cell Dev Biol* 18:81–105.
2. Palanivelu R, Tsukamoto T (2012) Pathfinding in angiosperm reproduction: Pollen tube guidance by pistils ensures successful double fertilization. *Wiley Interdiscip Rev Dev Biol* 1(1):96–113.
3. Qu LJ, Li L, Lan Z, Dresselhaus T (2015) Peptide signalling during the pollen tube journey and double fertilization. *J Exp Bot* 66(17):5139–5150.
4. Hiscock SJ, Allen AM (2008) Diverse cell signalling pathways regulate pollen-stigma interactions: The search for consensus. *New Phytol* 179(2):286–317.
5. Kim S, et al. (2003) Chemocyanin, a small basic protein from the lily stigma, induces pollen tube chemotropism. *Proc Natl Acad Sci USA* 100(26):16125–16130.
6. Wu HM, Wang H, Cheung AY (1995) A pollen tube growth stimulatory glycoprotein is deglycosylated by pollen tubes and displays a glycosylation gradient in the flower. *Cell* 82(3):395–403.
7. Cheung AY, Wang H, Wu HM (1995) A floral transmitting tissue-specific glycoprotein attracts pollen tubes and stimulates their growth. *Cell* 82(3):383–393.
8. Jékely G, Sung HH, Luque CM, Rørth P (2005) Regulators of endocytosis maintain localized receptor tyrosine kinase signaling in guided migration. *Dev Cell* 9(2):197–207.
9. Lemmon MA, Schlessinger J (2010) Cell signaling by receptor tyrosine kinases. *Cell* 141(7):1117–1134.
10. Shah K, Russinova E, Gadella TW, Jr, Willemse J, De Vries SC (2002) The *Arabidopsis* kinase-associated protein phosphatase controls internalization of the somatic embryogenesis receptor kinase 1. *Genes Dev* 16(13):1707–1720.
11. Robatzek S, Chinchilla D, Boller T (2006) Ligand-induced endocytosis of the pattern recognition receptor FLS2 in *Arabidopsis*. *Genes Dev* 20(5):537–542.
12. Geldner N, Hyman DL, Wang X, Schumacher K, Chory J (2007) Endosomal signaling of plant steroid receptor kinase BRI1. *Genes Dev* 21(13):1598–1602.
13. Le Roy C, Wrana JL (2005) Clathrin- and non-clathrin-mediated endocytic regulation of cell signalling. *Nat Rev Mol Cell Biol* 6(2):112–126.
14. Di Pietro SM, Dell'Angelica EC (2005) The cell biology of Hermansky-Pudlak syndrome: Recent advances. *Traffic* 6(7):525–533.
15. Price A, Wickner W, Ungermann C (2000) Proteins needed for vesicle budding from the Golgi complex are also required for the docking step of homotypic vacuole fusion. *J Cell Biol* 148(6):1223–1229.
16. Cabrera M, et al. (2009) Vps41 phosphorylation and the Rab Ypt7 control the targeting of the HOPS complex to endosome-vacuole fusion sites. *Mol Biol Cell* 20(7):1937–1948.
17. Ostrowicz CW, et al. (2010) Defined subunit arrangement and rab interactions are required for functionality of the HOPS tethering complex. *Traffic* 11(10):1334–1346.
18. Balderhaar HJ, Ungermann C (2013) CORVET and HOPS tethering complexes: Coordinators of endosome and lysosome fusion. *J Cell Sci* 126(Pt 6):1307–1316.
19. Radisky DC, Snyder WB, Emr SD, Kaplan J (1997) Characterization of VPS41, a gene required for vacuolar trafficking and high-affinity iron transport in yeast. *Proc Natl Acad Sci USA* 94(11):5662–5666.
20. Aoyama M, et al. (2012) Spatial restriction of bone morphogenetic protein signaling in mouse gastrula through the mVam2-dependent endocytic pathway. *Dev Cell* 22(6):1163–1175.
21. Geldner N, et al. (2009) Rapid, combinatorial analysis of membrane compartments in intact plants with a multicolor marker set. *Plant J* 59(1):169–178.
22. Bröcker C, et al. (2012) Molecular architecture of the multisubunit homotypic fusion and vacuole protein sorting (HOPS) tethering complex. *Proc Natl Acad Sci USA* 109(6):1991–1996.
23. Pols MS, ten Brink C, Gosavi P, Oorschot V, Klumperman J (2013) The HOPS proteins hVps41 and hVps39 are required for homotypic and heterotypic late endosome fusion. *Traffic* 14(2):219–232.
24. Sohn EJ, et al. (2003) Rha1, an Arabidopsis Rab5 homolog, plays a critical role in the vacuolar trafficking of soluble cargo proteins. *Plant Cell* 15(5):1057–1070.
25. Cui Y, et al. (2014) Activation of the Rab7 GTPase by the MON1-CCZ1 complex is essential for PVC-to-vacuole trafficking and plant growth in Arabidopsis. *Plant Cell* 26(5):2080–2097.
26. Ebine K, et al. (2014) Plant vacuolar trafficking occurs through distinctly regulated pathways. *Curr Biol* 24(12):1375–1382.
27. Johnsson N, Varshavsky A (1994) Split ubiquitin as a sensor of protein interactions in vivo. *Proc Natl Acad Sci USA* 91(22):10340–10344.
28. Stagljar I, Korostensky C, Johnsson N, te Heesen S (1998) A genetic system based on split-ubiquitin for the analysis of interactions between membrane proteins in vivo. *Proc Natl Acad Sci USA* 95(9):5187–5192.
29. Liu L, et al. (2010) An efficient system to detect protein ubiquitination by agroinfiltration in *Nicotiana benthamiana*. *Plant J* 61(5):893–903.
30. Miao Y, Li KY, Li HY, Yao X, Jiang L (2008) The vacuolar transport of aleurain-GFP and 2S albumin-GFP fusions is mediated by the same pre-vacuolar compartments in tobacco BY-2 and *Arabidopsis* suspension cultured cells. *Plant J* 56(5):824–839.
31. Vida TA, Emr SD (1995) A new vital stain for visualizing vacuolar membrane dynamics and endocytosis in yeast. *J Cell Biol* 128(5):779–792.
32. Hiscock S, Dewey F, Coleman JD, Dickinson H (1994) Identification and localization of an active cutinase in the pollen of *Brassica napus* L. *Planta* 193(3):377–384.
33. Shayk M, Kolattukudy PE (1977) Production of a novel extracellular cutinase by the pollen and the chemical composition and ultrastructure of the stigma cuticle of nasturtium (*Tropaeolum majus*). *Plant Physiol* 60(6):907–915.
34. Hiscock S, Bown D, Gurr S, Dickinson H (2002) Serine esterases are required for pollen tube penetration of the stigma in *Brassica*. *Sex Plant Reprod* 15(2):65–74.
35. Asensio CS, et al. (2013) Self-assembly of VPS41 promotes sorting required for biogenesis of the regulated secretory pathway. *Dev Cell* 27(4):425–437.
36. Lei ZH, et al. (2007) High-throughput binary vectors for plant gene function analysis. *J Integr Plant Biol* 49(4):556–567.
37. Boavida LC, McCormick S (2007) Temperature as a determinant factor for increased and reproducible in vitro pollen germination in *Arabidopsis thaliana*. *Plant J* 52(3):570–582.
38. Guan Y, Lu J, Xu J, McClure B, Zhang S (2014) Two mitogen-activated protein kinases, MPK3 and MPK6, are required for funicular guidance of pollen tubes in Arabidopsis. *Plant Physiol* 165(2):528–533.
39. Liu J, et al. (2013) Membrane-bound RLCKs LIP1 and LIP2 are essential male factors controlling male-female attraction in *Arabidopsis*. *Curr Biol* 23(11):993–998.
40. Guo Y, Qin G, Gu H, Qu LJ (2009) Dof5.6/HCA2, a Dof transcription factor gene, regulates interfascicular cambium formation and vascular tissue development in *Arabidopsis*. *Plant Cell* 21(11):3518–3534.
41. Liu J, et al. (2008) Targeted degradation of the cyclin-dependent kinase inhibitor ICK4/KRP6 by RING-type E3 ligases is essential for mitotic cell cycle progression during *Arabidopsis* gametogenesis. *Plant Cell* 20(6):1538–1554.
42. English JJ, Davenport GF, Elmayan T, Vaucheret D, Baulcombe C (1997) Requirement of sense transcription for homology-dependent virus resistance and trans-inactivation. *Plant J* 12(3):597–603.
43. Voinnet O, Rivas S, Mestre P, Baulcombe D (2003) An enhanced transient expression system in plants based on suppression of gene silencing by the p19 protein of tomato bushy stunt virus. *Plant J* 33(5):949–956.